Reactivity and Coordination Chemistry of Aromatic Carboxamide $RC(O)NH_2$ and Carboxylate Ligands: Properties of Pentaammineruthenium(II) and -(III) Complexes

Mei H. Chou, David J. Szalda,[1] Carol Creutz,* and Norman Sutin

Chemistry Department, Brookhaven National Laboratory, Upton, New York 11973-5000

Received December 14, 1993[⊗]

The pH dependences of the spectral and electrochemical properties of mononuclear carboxamido $(NH_3)_5RuNHC(O)R$ (R = Ph, 4-py-*N*-Me$^+$, 4-py-*N*-H$^+$) and carboxylato $(NH_3)_5RuOC(O)R$ (R = 4-py-*N*-Me$^+$) complexes of Ru(II) and Ru(III) in aqueous solution have been examined. In contrast to the carboxylate complex ($E_{1/2}$ = –0.053 V vs NHE), the deprotonated (–NHC(O)R$^-$) $Ru^{III/II}$ couples have rather negative reduction potentials, –0.25 (R = Ph), –0.23 (R = 4-py), and –0.13 (R = *N*-Me-4-py) V vs NHE, which are pH independent above the pK_a of the Ru(II) complex (pH 4–8 depending upon R). In contrast, the carboxamido–Ru(III) complexes are weak bases, being protonated only in strongly acidic solutions (e.g. 5 M $HClO_4$). From the structural work (d(Ru(III)–amido N) for R = *N*-Me-4-py is 1.998(9) Å) and the behavior of the ligand-to-metal charge-transfer bands in carboxamido–Ru(III) complexes, considerable oxygen πp–ruthenium(III) πd bonding is inferred. The electronic absorption spectra of carboxamido ruthenium(II) complexes, produced either by reduction of the corresponding Ru(III) complex at high pH or by direct reaction of $(NH_3)_5Ru(OH_2)^{2+}$ with the amide in 0.01 M NaOH, exhibit intense (ϵ (2.5–7) × 10^3 M^{-1} cm^{-1}) bands in the visible region arising from metal-to-ligand (aromatic ring) charge-transfer transitions. Rate and equilibrium constants for formation of the protonated Ru(II) amide complexes with R = Ph and R = 4-py-*N*-Me$^+$ at 25 °C and 0.1 M ionic strength are (7 ± 1) × 10^{-2} M^{-1} s^{-1} and 2 × 10^{-3} M^{-1} for the first R and 1.2 × 10^{-2} M^{-1} s^{-1} and 2.0 × 10^{-3} M^{-1} for the second, respectively. For the carboxylate under similar conditions, the values 0.6 M^{-1} s^{-1} and 0.6 M^{-1} are obtained. The free amide ligand *N*-methylisonicotinamide triflate undergoes rapid alkaline hydrolysis, yielding *N*-methylisonicotinate and ammonia under exceptionally mild conditions (2-h half-life in 0.01 M NaOH, 15 °C). At 15, 25, and 35 °C and 1 M ionic strength the rate of hydrolysis (monitored by UV–vis spectroscopy) is first order in the amide concentration. The dependence on hydroxide ion is between first and second order. Thus at 25 °C, the second-order rate constant increases from 1.43 × 10^{-2} M^{-1} s^{-1} at 0.01 M OH^- to 3.08 × 10^{-2} M^{-1} s^{-1} at 0.05 M OH^-. The structures of the Ru(III) carboxamide $[(NH_3)_5Ru(C_7N_2H_8O)](ClO_4)_3$, R = 4-py-*N*-Me$^+$, and of the *N*-pyridyl-bonded Ru(II) complex of isonicotinamide $(NH_4)[Ru(NH_3)_5(C_6N_2H_6O)](PF_6)_3$ are reported.

Introduction

The chemistry of the metal–NHC(O) linkage is of interest in its own right and in the context of metal ion–peptide chemistry.[2,3] The solution chemistry of carboxamide complexes of cobalt(III), rhodium(III), and, recently, platinum(II) have received attention in the literature.[4] Carboxamido–ruthenium(III) complexes were first discovered as products of the hydrolysis of the parent nitrile,[5-7] and the hydrolysis reaction is generally a superior synthetic route. Chelated glycinamide(ruthenium) complexes "anchored" by an NH_2 bond to the metal were found to exhibit a complex isomerism, with the N or the O of the carboxamide function binding the ruthenium,[8] depending upon acidity and the oxidation state of the metal; one of the –NHC(O) bonded isomers has been structurally characterized.[9] Recently –NHC(O) was found to serve as part of a bridging ligand in binuclear Fe(II)–Ru(III) mixed-valence species.[7] Our interest in the coordination chemistry of carboxamido ligands was stimulated by the possibility of using these ligands as the lead-in groups of extended bridges between Ru(II) and Ru(III) centers.[10] Our work with the binuclear systems raised some issues concerning the properties of the $Ru(NH_3)_5$–NHC(O)R moiety. Thus we have repeated and extended some physical measurements in the literature and characterized the structure of one complex of this family. We have also extended our preliminary studies[11] of the Ru(II) complexes and characterized a related carboxylate complex. The results of these studies are reported here.

Experimental Section

Materials and Methods. Isonicotinamide, 4-cyanopyridine, cyanobenzene, benzamide, silver trifluoromethanesulfonate, and ammonium hexafluorophosphate were used as obtained from Aldrich. Trifluoromethanesulfonic (triflic) acid was purchased from Alfa and hexaammineruthenium(III) trichloride, from Matthey-Bishop, Inc. *N*-Methyl-4-cyanopyridinium iodide was prepared from methyl iodide and 4-cyanopyridine as described by Huang et al.[7] Isonicotinamide (5 g, Aldrich) was alkylated with methyl iodide (25 mL, Aldrich) at 35 °C (reaction time, 1 week). The resulting yellow solid iodide was recrystallized from 50 °C ethanol/water (2:1) and then converted to the triflate salt by treatment with methanolic silver triflate (Aldrich). The triflate was recrystallized from methanol/ether.

The methylated analogue of isonicotinic acid was prepared similarly, but was obtained in only about 10% yield. Ultimately hydrolysis of the amide was found to be a superior route: 1.15 g (4 mmol) of $(H_2NC(O)$-4-py-*N*-$CH_3)(CF_3SO_3)$ was dissolved in 6 mL of 1 M NaOH and left in the dark at room temperature for 2 h. The solution was then neutralized to pH 5.4 by dropwise addition of 1 M triflic acid and then evaporated to dryness on a rotary evaporator. (Failure to neutralize the

⊗ Abstract published in *Advance ACS Abstracts*, March 15, 1994.

(1) To whom questions concerning the X-ray crystallography should be directed. Permanent address: Department of Natural Science, Baruch College, Manhattan, NY 10010.
(2) Sigel, H.; Martin, R. B. *Chem. Rev.* **1982**, *82*, 385–426.
(3) Takasaki, B. K.; Kim, J. H.; Rubin, E.; Chin, J. *J. Am. Chem. Soc.* **1993**, *115*, 1157–1159.
(4) Woon, T. C.; Fairlie, D. P. *Inorg. Chem.* **1992**, *31*, 4069–4074.
(5) Zanella, A. W.; Ford, P. C. *Inorg. Chem.* **1975**, *14*, 42–47.
(6) Diamond, S. E.; Grant, B.; Tom, G. M.; Taube, H. *Tetrahedron Lett.* **1974**, 4025–4028.
(7) Huang, H.-Y.; Chen, W.-J.; Wang, C.-C.; Yeh, A. *Inorg. Chem.* **1991**, *30*, 1862–1868.
(8) Ilan, Y.; Taube, H. *Inorg. Chem.* **1983**, *22*, 1655–1664.
(9) Ilan, Y.; Kapon, M. *Inorg. Chem.* **1986**, *25*, 2350–2354.
(10) Chou, M. H.; Creutz, C.; Sutin, N. *Inorg. Chem.* **1992**, *31*, 2318–2327.
(11) Chou, M. H.; Brunschwig, B. S.; Creutz, C.; Sutin, N.; Yeh, A.; Chang, R. C.; Lin, C.-T. *Inorg. Chem.* **1992**, *31*, 5347–5348.

0020-1669/94/1333-1674$04.50/0

solution resulted in formation of a black tar when the solution volume was reduced.) The dry white solid, a mixture of OC(O)-4-py-*N*-CH_3 and sodium triflate, was dissolved in 5 mL of methanol, filtered, loaded onto a 12-cm long column (1.5-cm diameter) of 40 Å, 35–70 mesh silica gel (Aldrich), and eluted with methanol. The first 100 mL contained the inorganic salt and were discarded. The following 300 mL contained the desired zwitterion and were combined and evaporated to dryness to yield 0.4 g of amide-free material as verified by TLC on fluorescent-indicator impregnated silica (Polygram Sil G/UV-254, Alltech).

The carboxylate-bound complex of OC(O)-4-py-*N*-CH_3 was prepared from 0.5 mL of 1.67 M L and 0.33 M $[(NH_3)_5RuOH_2](CF_3SO_3)_3$ at pH 3. To the deaerated mixture was added $(NH_3)_5RuOH_2^{2+}$ (prepared by amalgamated-zinc reduction of the Ru(III) complex[10]) to give 0.038 M Ru(II). The solution became blue. The mixture was left for an hour, then opened to and mixed with air to give a gold-colored solution of the Ru(III) complex. Cooling of the filtered product solution overnight at 4 °C gave a small crop of the triflate salt, and more solid formed when triflic acid was added to the filtrate from the first crop. The solid was washed with methanol and ether and gave a satisfactory Ru analysis for $[(NH_3)_5Ru(OC(O)\text{-}4\text{-}py\text{-}N\text{-}CH_3)](CF_3SO_3)_3$. UV–vis: λ_{max}, 272 nm; ϵ, 5.0×10^3 M^{-1} cm^{-1}.

The benzamide complex $[(NH_3)_5Ru^{III}(NHC(O)Ph)](PF_6)_2$, was prepared following Zanella and Ford.[5] The (carboxamido)ruthenium(III) complexes, $(NH_3)_5Ru(NHC(O)\text{-}4\text{-}py\text{-}N\text{-}H)(ClO_4)_3$ and $(NH_3)_5Ru(NHC(O)\text{-}4\text{-}py\text{-}N\text{-}Me)(ClO_4)_3$, were prepared by the hydrolysis of the corresponding nitrile–ruthenium(III) complexes,[7] which were generated by peroxy disulfate oxidation of the PF_6^- or ClO_4^- salts of the ruthenium(II) nitrile complexes.[12,13] These complexes were characterized by UV–vis and small-scale cation exchange chromatography (≥95% single component) on Sephadex C-25. Crystals of $[(NH_3)_5Ru^{III}(NHC(O)\text{-}4\text{-}py\text{-}N\text{-}Me)](ClO_4)_3$ were grown by leaving a solution of *ca.* 10 mg of the perchlorate salt dissolved in 1.5 mL of water in an evacuated desiccator over Drierite for several days. Crystals of $(NH_4)[(NH_3)_5Ru^{II}(4\text{-}pyC(O)NH_2)](PF_6)_3$ (grown at 4 °C) were collected from an aqueous solution of NH_4PF_6 used in an unsuccessful attempt to grow crystals of the mixed-valence μ-isonicotinamido complex.[10]

Caution! Perchlorate salts of ruthenium ammines may detonate readily and should be avoided whenever possible! They should be handled only in small quantities and with appropriate precautions (gloves, explosion shield, etc.).

UV-vis spectra were determined with Cary 210 or Hewlett-Packard 8452A diode array spectrometers and NMR spectra on a Bruker AM-300 300-MHz spectrometer.

Electrochemical experiments (cyclic voltammetry and differential pulse voltammetry) were carried out with a BAS electrochemical analyzer, with a glassy-carbon working electrode, a platinum-wire auxiliary electrode, and a saturated calomel (SCE) reference electrode in a conventional H-cell. For the studies of pH dependences, a cell equipped with a working-cell extension for a pH electrode was used and 4 mM phosphate, 0.1 or 0.5 M KCF_3SO_3 and millimolar ruthenium(III) complex were adjusted to the desired pH with NaOH (0.1 M) or CF_3SO_3H (0.1 or 1 M). In CH_3CN solvent, tetrabutylammonium hexafluorophosphate (0.1 M) was used as supporting electrolyte for the electrochemical experiments. No compensation for IR drop was made.

Two approaches were used in the spectroscopic study of Ru(II)–carboxamido complexes in solution: In the first, the solutions were produced by reduction of the Ru(III) complex. (The Ru(III) solutions always contained millimolar amounts of acid.) At pH ≤ 7, V(II) or $Ru(NH_3)_6^{2+}$ in dilute acid (1–5 mM) or acetate buffer (0.1 M, pH 4–6) were used. The V(II) or $Ru(NH_3)_6^{2+}$ stock solutions were generated by the reduction of VO^{2+} or $Ru(NH_3)_6^{3+}$ solutions with amalgamated zinc (Zn–Hg). Sodium dithionite (MCB or Fisher, weighed out and dissolved immediately in deaerated aqueous buffer) was used as a reducant in the pH range 3–11. The spectra of the product solutions were scanned repeatedly with the diode array spectrometer. In the second approach, the fact that complexation of the amido function to Ru(II) becomes more favorable as pH increases (below the pK_a of $(NH_3)_5Ru(OH_2)^{2+}$; values of the aqua ion pK have been given as 12.3[14] and 13.1 ± 0.1 (ionic strength 0.45 to 1.0 M[15])) was exploited: $(NH_3)_5Ru(OH_2)^{2+}$, prepared by reduction of the Ru(III) complex with Zn–Hg, was added to 1-cm cuvettes containing the desired concentrations of amide, electrolyte, and buffer or NaOH. These experiments suffered from complications in the chemistry of ruthenium ammines and of the ligand $NH_2C(O)$-4-py-*N*-Me^+ in alkaline solution (vide infra).

Standard syringe techniques were used in all these studies, with argon as blanket gas.

Ammonia was determined potentiometrically with an ammonia specific electrode (Orion, Model 95-10).

Table 1. Crystallographic Data for $[(NH_3)_5Ru^{III}(C_7N_2H_8O)](ClO_4)_3$ and $(NH_4)[(NH_3)_5Ru^{II}(C_6N_2H_6O)](PF_6)_3$

formula	$[(NH_3)_5Ru(C_7N_2H_8O)](ClO_4)_3$	$(NH_4)[(NH_3)_5Ru(C_6N_2H_6O)](PF_6)_3$
a, Å	12.402(1)	8.603(1)
b, Å	7.9028(6)	27.135(3)
c, Å	22.486(3)	10.6497(8)
β, deg		93.138(8)
V, Å^3	2203.9(4)	2482.4(7)
Z	4	4
fw	620.73	761.28
space group	*Pnma*	$P2_1/c$
ρ(calcd) g cm^{-3}	1.871	2.037
λ,[a] Å	1.5418 (Cu Kα)	1.5418 (Cu Kα)
μ, cm^{-1}	100	86.6
transm coeff	0.1540–0.4385	0.2010–0.4824
R[b]	0.067	0.066
R_w[b]	0.087	0.076
max shift/error final cycle	≤0.03	≤0.02
T, K	296	295

[a] Graphite monochromatized. [b] $R = \sum||F_o| - |F_c||/\sum|F_o|$; $R_w = \{\sum[w(|F_o| - |F_c|)^2]/\sum[w|F_o|^2]\}^{1/2}$.

Crystal Structure Determinations. The crystals of $[(NH_3)_5Ru^{III}(NHC(O)\text{-}4\text{-}py\text{-}N\text{-}Me)](ClO_4)_3$ were yellow-brown needles. A crystal 0.10 × 0.14 × 0.57 mm was coated with petroleum jelly and sealed inside a glass capillary. Diffraction data indicated systematic absences $h0l$, $h + l = 2n + 1$, and $hk0$, $k = 2n + 1$, consistent with space groups *Pmnb* and $P2_1nb$ (nonstandard settings *Pnma* (No. 62, D_{2h}^{16})[16] and $Pna2_1$ (No. 33, C_{2v}^9).[17] Solution and refinement of the structure indicated the centrosymmetric space group as the correct choice, so the crystal parameter and intensity data were transformed to *Pnma*, the standard setting, and all data reported here refer to this space group.

A reddish brown crystal of $(NH_4)[(NH_3)_5Ru^{II}(4\text{-}pyC(O)NH_2)](PF_6)_3$, 0.07 × 0.15 × 0.42 mm, was coated with petroleum jelly and sealed inside a glass capillary. Diffraction data indicated monoclinic symmetry with systematic absences $h0l$, $l = 2n + 1$, and $0k0$, $k = 2n + 1$, consistent with space group $P2_1/c$ (No. 14, C_{2h}^5).[18]

Crystal data and information about data collection are given in Tables 1 and S1.

The structures were solved[19] by standard Patterson heavy-atom methods. In the least-squares refinements,[19] anisotropic temperature parameters were used for all of the non-hydrogen atoms (except for the F atoms of the disordered PF_6^- groups) and the quantity $\sum w(|F_o| - |F_c|)^2$ was minimized. Hydrogen atoms on the ligands were placed at calculated positions (X–H = 0.95 Å) and were allowed to "ride" on the C or N to which they were attached. A common isotropic thermal parameter was refined for all of these hydrogen atoms. (Hydrogen atoms of the ammonium cation and the amide group in the Ru(II) complex were not included.) The largest peak on the final difference Fourier maps was 1.2 e$^-$/Å^3 located 1 Å from the ruthenium atom in $[(NH_3)_5Ru^{III}(NHC(O)\text{-}4\text{-}py\text{-}N\text{-}Me)](ClO_4)_3$ and 0.78 e$^-$/Å^3 located near the disordered PF_6^- anion in $(NH_4)[(NH_3)_5Ru(4\text{-}pyC(O)NH_2)](PF_6)_3$.

Selected interatomic distances and angles are given in Table 2. Final non-hydrogen atom positional parameters are listed in Table S9.

Results

Description of the Structures. The atom numbering schemes

(12) Clarke, R. E.; Ford, P. C. *Inorg. Chem.* **1970**, *9*, 495–499.
(13) Clarke, R. E.; Ford, P. C. *Inorg. Chem.* **1970**, *9*, 227–235.
(14) Lim, H. S.; Barclay, D. J.; Anson, F. C. *Inorg. Chem.* **1972**, *11*, 1460–1466.
(15) Kuehn, C. G.; Taube, H. *J. Am. Chem. Soc.* **1976**, *98*, 689–702.
(16) *International Tables for X-ray Crystallography*, 3rd ed.; Kynoch Press: Birmingham, UK, 1969; Vol. I, p 151.
(17) *International Tables for X-ray Crystallography*, 3rd ed.; Kynoch Press: Birmingham, UK, 1969; Vol. I, p 119.
(18) *International Tables for X-ray Crystallography*, 3rd ed.; Kynoch Press: Birmingham, UK, 1969; Vol. I, p 99.
(19) Sheldrick, G. M. SHELX 76: Crystal Structure Refinement Program. Cambridge University, Cambridge, England, 1976.

Table 2. $[(NH_3)_5Ru(NHC(O)4\text{-py-}N\text{-Me})](ClO_4)_3$ and $(NH_4)[(NH_3)_5Ru(py\text{-}4\text{-}C(O)NH_2)](PF_6)_3$ Bond Distances (Å) and Angles (deg)[a]

$[(NH_3)_5Ru^{III}(NHC(O)4\text{-py-}N\text{-Me})](ClO_4)_3$

Ruthenium–Ligand Distances

Ru–N(1)	1.998(9)	Ru–N(2)	2.105(8)
Ru–N(4)	2.123(8)	Ru–N(6)	2.148(10)

Ruthenium–Ligand Angles

N(1)–Ru–N(2)	90.5(3)	N(2)–Ru–N(4)	178.7(3)
N(1)–Ru–N(4)	89.5(3)	N(2)–Ru–N(6)	88.5(3)
N(1)–Ru–N(6)	178.5(4)	N(4)–Ru–N(4′)	88.3(3)
N(2)–Ru–N(2′)	90.9(3)	N(4)–Ru–N(6′)	91.6(3)

Deprotonated *N*-Methylisonicotinamide Distances

N(1)–C(1)	1.325(15)	C(13)–N(14)	1.285(19)
C(1)–O(1)	1.236(15)	N(14)–C(15)	1.325(19)
C(1)–C(11)	1.508(16)	C(15)–C(16)	1.347(20)
C(11)–C(12)	1.393(18)	C(16)–C(11)	1.379(17)
C(12)–C(13)	1.364(20)	N(14)–C(14)	1.518(17)

Deprotonated *N*-Methylisonicotinamide Angles

Ru–N(1)–C(1)	126.3(8)	C(11)–C(12)–C(13)	120(1)
N(1)–C(1)–O(1)	124(1)	C(12)–C(13)–N(14)	123(1)
N(1)–C(1)–C(11)	119(1)	C(13)–N(14)–C(14)	121(1)
O(1)–C(1)–C(11)	117(1)	C(13)–N(14)–C(15)	119(1)
C(1)–C(11)–C(12)	117(1)	C(14)–N(14)–C(15)	120(1)
C(1)–C(11)–C(16)	127(1)	N(14)–C(15)–C(16)	120(1)
C(12)–C(11)–C(16)	116(1)	C(15)–C(16)–C(11)	121(1)

$(NH_4)[(NH_3)_5Ru^{II}(py\text{-}4\text{-}C(O)NH_2)](PF_6)_3$

Ruthenium–Ligand Distances

Ru–N(14)	2.049(7)	Ru–N(2)	2.141(9)
Ru–N(3)	2.141(8)	Ru–N(4)	2.122(8)
Ru–N(5)	2.140(8)	Ru–N(6)	2.171(9)

Ruthenium–Ligand Angles

N(14)–Ru–N(2)	90.5(3)	N(2)–Ru–N(6)	88.5(3)
N(14)–Ru–N(3)	90.7(3)	N(3)–Ru–N(4)	90.3(3)
N(14)–Ru–N(4)	93.2(3)	N(3)–Ru–N(5)	178.7(3)
N(14)–Ru–N(5)	90.5(3)	N(3)–Ru–N(6)	89.2(3)
N(14)–Ru–N(6)	179.0(3)	N(4)–Ru–N(5)	89.1(3)
N(2)–Ru–N(3)	89.3(4)	N(4)–Ru–N(6)	87.8(3)
N(2)–Ru–N(4)	176.3(3)	N(5)–Ru–N(6)	89.6(3)
N(2)–Ru–N(5)	91.2(4)		

Isonicotinamide Distances

N(1)–C(1)	1.322(12)	C(13)–N(14)	1.340(12)
C(1)–O(1)	1.242(11)	N(14)–C(15)	1.364(11)
C(1)–C(11)	1.512(12)	C(15)–C(16)	1.384(13)
C(11)–C(12)	1.374(13)	C(16)–C(11)	1.359(13)
C(12)–C(13)	1.380(12)		

Isonicotinamide Angles

Ru–N(14)–C(13)	119.8(6)	Ru–N(14)–C(15)	123.3(7)
N(1)–C(1)–O(1)	123.5(9)	C(11)–C(12)–C(13)	120.8(9)
N(1)–C(1)–C(11)	118.0(9)	C(12)–C(13)–N(14)	122.7(9)
O(1)–C(1)–C(11)	118.5(8)	C(13)–N(14)–C(15)	116.9(8)
C(1)–C(11)–C(12)	117.2(9)	N(14)–C(15)–C(16)	121(1)
C(1)–C(11)–C(12)	126.1(9)	C(15)–C(16)–C(11)	121.8(9)
C(12)–C(11)–C(16)	116.6(9)		

[a] The mirror plane relates O(12) and O(11), N(2′) and N(2), and N(4′) to N(4).

are shown in the ORTEP figures of the cations in Figure 1. In $[(NH_3)_5Ru^{III}(NHC(O)\text{-}4\text{-py-}N\text{-Me})](ClO_4)_3$, the coordination geometry of the Ru(III) center is effectively octahedral with five ammonias and the nitrogen of the deprotonated carboxamide serving as ligands. The Ru^{III}–NHC(O) bond (1.998(9) Å) is much shorter than the Ru–NH_3 bonds (2.121(8)Å, average). The Ru–O cis arrangement is stabilized by intramolecular hydrogen bonding of the carbonyl oxygen to the ammine hydrogens (see supplementary material). The –NHC(O)-4-py ligand is constrained to lie on a crystallographic mirror plane, but the large thermal parameters for C(12), C(13), and C(14) (see Figure 1) indicate that these atoms may be slightly out of this plane. The coplanarity of the RuNHC(O)– and pyridyl portions of the ligand is noteworthy.

The structure of $(NH_4)[(NH_3)_5Ru(4\text{-py}C(O)NH_2)](PF_6)_3$ consists of Ru(II) coordinated octahedrally to five ammonias and the pyridine nitrogen of the neutral isonicotinamide ligand. The Ru(II)–pyridine distance (Ru–N(14)) is 2.049(7) Å. The Ru–NH_3 bond trans to the isonicotinamide is longer (2.171(9) Å) than the other Ru–NH_3 bonds (2.136(8) Å, average). The dihedral angle between the pyridine ring and the amide group of the isonicotinamide is 10.9°. The crystal lattice conains three PF_6^- anions and an NH_4^+ cation. (Proposed hydrogen bonds of NH_4^+ with the O of the amide and the fluorines of the anions are given in the supplementary material. Intermolecular hydrogen bonds between the amide groups of two symmetry-related complexes are also given there.)

Hydrolysis of *N*-Methylated Isonicotinamide. Although rates of amide hydrolysis are usually insignificant at room temperature,[20–23] problems with irreproducibility in the kinetics of binding of $(NH_3)_5Ru(OH_2)^{2+}$ to $NH_2C(O)$-4-py-*N*-Me^+ in alkaline solution led us to investigate the hydrolysis of the ligand (eq 1). In preliminary work, the amide hydrolysis was followed

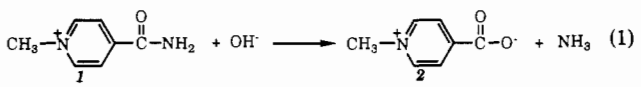

(1)

by ^1H NMR: with 0.01 M NaOD and 0.01 M **1** dissolved in D_2O, all three reactant peaks (δ 8.77 (d, 2H), 8.16 (d, 2H), 4.26 (s, 3 H)) diminished in intensity and developed the corresponding product peaks (verified by comparison with a sample prepared by *N*-methylation of isonicotinic acid: δ 8.65 (d, 2H), 8.06 (d, 2H), 4.23 (s, 3 H)); 0.0097 M ammonia was produced. (H/D exchange of the lowest field protons, presumably at the 2-position, occurred more slowly.) The yield of ammonia was 105 ± 5% based on amide taken with 1.00 mM amide and 0.01, 0.03, and 0.05 M NaOH at 25 °C. Systematic kinetic studies with 0.3 mM amide were performed by following the absorbance decrease at 265 nm in a 1-cm cell (**1**, λ_{max} = 266 nm, $\epsilon_{max} = 4.3 \times 10^3$ M^{-1} cm^{-1}; **2**, λ_{max} = 262 nm, $\epsilon_{max} = 3.7 \times 10^3$ M^{-1} cm^{-1}). Plots of $\log(A_t - A_\infty)$ were linear and pseudo-first-order rate constants k_{obs} were obtained from them. Second-order rate constants (k_{obs}/[OH^-]) are plotted against [OH^-] in Figure 2. In preliminary runs with 0.1 M ionic strength (potassium triflate) the rates were about 40% faster than those in Figure 2, and a new absorption feature (either the deprotonated amide, an ion pair with OH^- or a pseudo-base) was observed at 306 nm in the reactants' spectra when [OH^-] ≥ 0.03 M. The 306-nm band was not observed in the μ = 1 M medium.

The dependence of the rate on [OH^-] is between first and second order, behavior similar to that reported[24] for acetanilide hydrolyses. The term first order in [OH^-] has been attributed to the addition of OH^- to the carbonyl carbon, and the second-order term, to deprotonation of this adduct. Hydrolysis may occur via either the protonated or deprotonated intermediate, and depending on the relative rates of the various steps, complex hydroxide ion dependences may result.[24,25] Because of the complexity of the rate law, detailed discussion of the temperature dependence of the rate is not warranted. It is, however, obvious that the activation energy(ies) are much smaller than those reported[24] for substituted benzamides.

(20) Meloche, I.; Laidler, K. J. *J. Am. Chem. Soc.* **1951**, *73*, 1712–1714.
(21) Bender, M. L.; Ginger, R. D. *J. Am. Chem. Soc.* **1955**, *77*, 348–351.
(22) Favini, G. *Rend. Ist. Lomb. Sci., Part I* **1957**, *91*, 162–169. (*Chem. Abstr.* **1958**, *52*, 11539e; *Beilsteins Handbuch der Organischen Chemie*, 4 Aufl.; Springer: Berlin, 1979; Drittes and Viertes Erganzungswerk, Bänder 22, 46, 527.)
(23) Brown, R. S.; Bennet, A. J.; Slebocka-Tilk, H. *Acc. Chem. Res.* **1992**, *25*, 481–488.
(24) Bender, M. L.; Thomas, R. J. *J. Am. Chem. Soc.* **1961**, *83*, 4183–4189.
(25) In reality, the plots in Figure 2 are slightly concave downward, consistent with a kinetically complex fate for the tetrahedral OH^--adduct. The possibility that the pseudobase (hydroxide solution to the 3-/5-carbon of isonicotinamide) is an intermediate in the hydrolysis cannot be ignored.

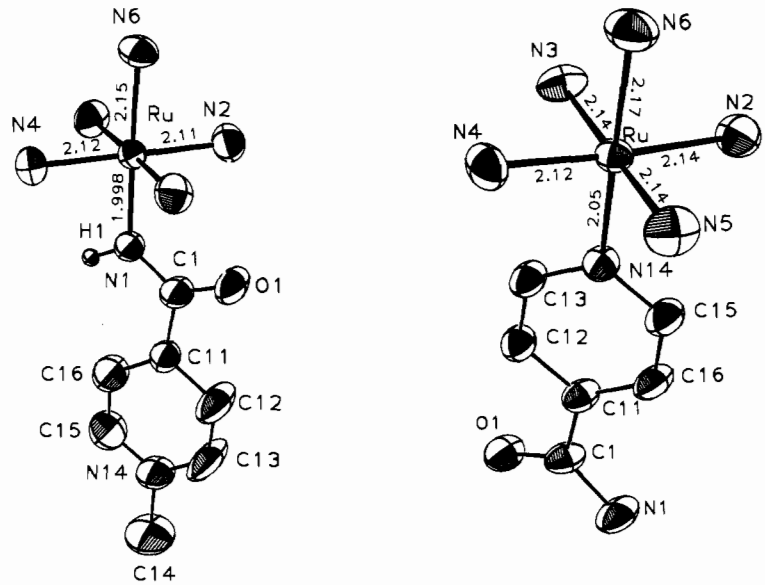

Figure 1. (a) Left: View of the $(NH_3)_5Ru^{III}(NHC(O)4\text{-py})^{2+}$ cation and the atom-labeling scheme. N(6), Ru, and all of the atoms in the NHC(O)-4-py ligand lie on a crystallographic mirror plane. Two ammonia ligands N(2) and N(2′) (which is related to N(2) by the mirror plane) form intramolecular hydrogen bonds to the oxygen atom of the carboxamido group. (b) Right: View of the of the $(NH_3)_5Ru^{II}(4\text{-pyC(O)NH}_2)^{2+}$ cation. The amide group makes a 10.7° angle with the plane of the pyridine ring. The thermal ellipsoids are at the 50% probability level and hydrogen atoms are omitted for clarity. Metal–ligand bond distances are in angstroms.

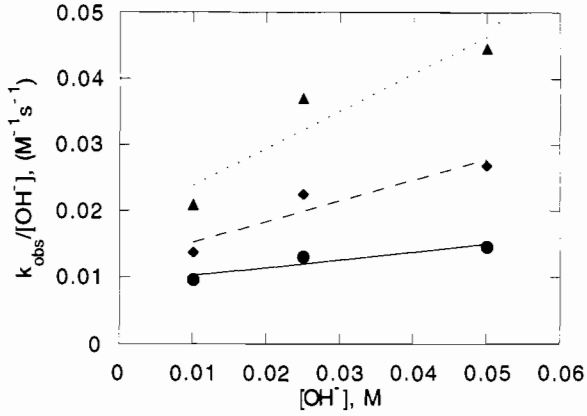

Figure 2. Base hydrolysis of *N*-methylisonicotinamide triflate at 1.0 M ionic strength (Na_2SO_4) at 15 (circles), 25 (diamonds), and 35 °C (triangles). Each point is the average from 2–3 replicate runs agreeing within ±7%. The lines are least-squares fit to the data points which actually deviate concave from the lines.

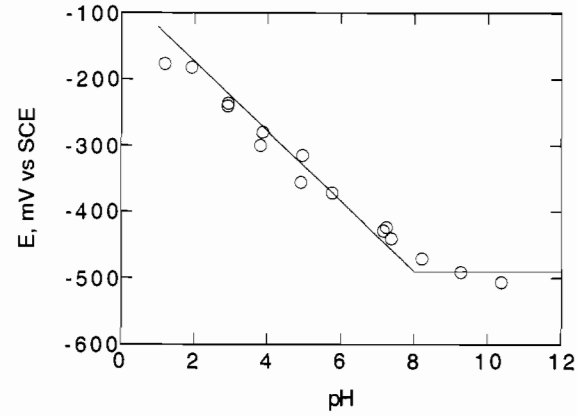

Figure 3. pH dependence of potential for the pentaammine(*N*-benzamide)ruthenium couple in 0.1 M potassium triflate at 22 ● 2 °C. The solid lines are imposed for $E_{1/2}(NH_3)_5Ru(NHC(OH)Ph)^{3+/2+}$ = –115 mV *vs* SCE and $E_{1/2}$ $(NH_3)_5Ru(NHC(O)Ph)^{2+/+}$ = –490 mV *vs* SCE and pK_a values of 0.9 for $(NH_3)_5Ru(NHC(OH)Ph)^{3+}$ and 8.0 for $(NH_3)_5$-$Ru(NHC(OH)Ph)^{2+}$.

The rate of hydrolysis of *N*-methylated nicotinamide in 0.05 M NaOH (μ = 1.0 M, Na_2SO_4, 25 °C) was about five times slower than that of the 4-isomer.

Electrochemistry. Since the carboxamido complexes undergo protonation and the Ru(II) complexes are more basic than their Ru(III) counterparts, the electrochemical response of complexes in this family is pH dependent (Scheme 1). (Here and elsewhere[10] protonation at oxygen is assumed.) The cyclic voltammograms were reversible only on relatively rapid timescales because the reduced species aquate fairly rapidly.[11] The pH-dependence of the benzamido couple is shown in Figure 3. Analysis of the electrochemical data yields $E_{1/2}^{amH}$ = +0.127 V *vs* NHE for the $(NH_3)_5Ru(NHC(OH)Ph)^{3+/2+}$ couple and $E_{1/2}^{am}$ = –0.258 V *vs* NHE for the $(NH_3)_5Ru(NHC(O)Ph)^{2+/+}$ couple, with $pK_{amH^{III}}$ = 0.9[5] and $pK_{amH^{II}}$ = 8.0.

For R = 4-py-*N*-Me^+, quasireversible cyclic voltammograms with $E_{pc} - E_{pa}$ = 90 mV (v = 5 V/s) were obtained at pH 4.5 and above. At pH 3.3, quasireversible behavior was observable with a sweep of 10 V/s. At lower pH values, the anodic component was lost, because of rapid aquation of the Ru(II) complex.[11] The pH dependence of the potential is shown in Figure 4. The solid lines are imposed for $E_{1/2}$ = –370 mV *vs* SCE for $(NH_3)_5$-$Ru(NHC(O)\text{-4-py-}N\text{-Me})^{3+/2+}$ and $pK_{amH^{II}}$ = 4.2. From the hydrogen ion dependence of the UV spectrum of the Ru(III) complex, it is inferred to be half-protonated in 4.5 M perchloric or triflic acid; thus $pK_{amH^{III}}$ = *ca* –0.3.

Scheme 1

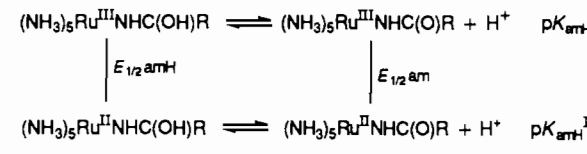

The $(NH_3)_5Ru(NHC(O)\text{-4-py})^{2+/+}$ system is the most complicated examined here because of the possibility of pyridyl protonation (Scheme 2) in addition to the equilibria in Scheme 1 and isomerization[11] Scheme 3. (Note that, in Scheme 2, the NHC(O) group is O-protonated for Ru(II), but not for Ru(III).) From the pH-dependence of the 386- (deprotonated pyridyl) and 356-nm (protonated pyridyl) peak intensities, $pK_{pyH^{III}}$ = 4.3 ± 0.3 at 22 ± 2 °C in 0.5 M potassium triflate was obtained (free isonicotinamide, 3.61[26]). Electrochemical data for R = 4-py are presented in Figure 5. Quasireversible cyclic voltammograms

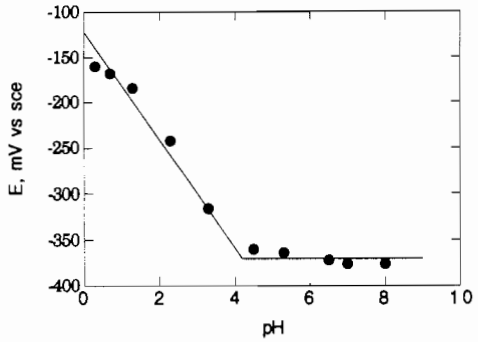

Figure 4. pH dependence of potential for the *N*-methylisonicotinamido couple in 0.5 M potassium triflate at 22 ± 2 °C. The solid lines are imposed for $E_{1/2}(NH_3)_5Ru(NHC(O)py\text{-}N\text{-}Me)^{3+/2+} = -370$ mV *vs* SCE and pK_a = 4.2 for $(NH_3)_5Ru^{II}(NHC(OH)py\text{-}N\text{-}Me)^{3+}$. From the dependence of the UV spectrum of the Ru(III) complex on acidity, pK_a = ca. –0.3 for $(NH_3)_5Ru^{III}(NHC(OH)py\text{-}N\text{-}Me)^{4+}$.

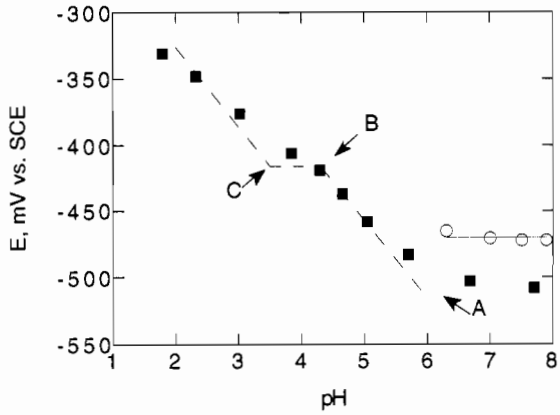

Figure 5. pH dependence of potential for the isonicotinamido couple in 0.1 M potassium triflate containing 0.01 M acetate and 1 mM Ru(III) complex at 22 ± 2 °C obtained from cyclic voltammetry. The open circles are values of $E_{av} = (E_{pc} + E_{pa})/2$; the solid squares are E_{pc} values obtained at 0.3 V/s sweep rates. The solid lines are imposed for $E_{pc}((NH_3)_5Ru(NHC(O)py)^{3+/2+} = -500$ mV *vs* SCE with the following pK_a values: A, 6.2 for $(NH_3)_5Ru^{II}(NHC(OH)py)^{2+}$; B (from the dependence of the UV spectrum of the Ru(III) complex on acidity), 4.3 for $(NH_3)_5Ru^{III}(NHC(O)pyH)^{3+}$; C, 3.5 for $(NH_3)_5Ru^{II}(NHC(OH)\text{-}pyH)^{3+}$ (from the pH dependence of the isomerization yields.[11] The plot is intended to illustrate the consistency of pK_a values (A–C) inferred from other measurements with the electrochemical observations.

Scheme 2

$$(NH_3)_5Ru^{III}NHC(O)\text{-}4\text{-}pyH^{3+} \rightleftharpoons (NH_3)_5Ru^{III}NHC(O)\text{-}4\text{-}py^{2+} + H^+ \quad pK_{pyH}{}^{III} = 4.3$$

$$(NH_3)_5Ru^{II}NHC(OH)\text{-}4\text{-}pyH^{3+} \rightleftharpoons (NH_3)_5Ru^{II}NHC(OH)\text{-}4\text{-}py^{2+} + H^+ \quad pK_{pyH}{}^{II} \sim 3$$

Scheme 3

$$(NH_3)_5Ru^{II}NHC(O)\text{-}4\text{-}py^{+} + H^+ \rightleftharpoons (NH_3)_5Ru^{II}NHC(OH)\text{-}4\text{-}py^{2+} \quad pK_{a,arH}{}^{II} = 6.2$$

$$(NH_3)_5Ru^{II}NHC(OH)\text{-}4\text{-}py^{2+} \longrightarrow (NH_3)_5Ru^{II}\text{-}4\text{-}pyC(O)NH_2{}^{2+}$$

$$(NH_3)_5Ru^{II}NHC(OH)\text{-}4\text{-}py^{2+} + H^+ \rightleftharpoons (NH_3)_5Ru^{II}NHC(OH)\text{-}4\text{-}pyH^{3+}$$

$$(NH_3)_5Ru^{II}NHC(OH)\text{-}4\text{-}pyH^{3+} \longrightarrow Ru(NH_3)_5(OH_2)^{2+} + Hpy\text{-}4\text{-}C(O)NH_2{}^{+}$$

with $E_{pc} - E_{pa}$ = 70 mV (v = 0.1 V/s) were obtained at pH ≥7 in 0.1 M potassium triflate. From $(E_{pc} + E_{pa})/2$, $E_{1/2}{}^{am} = -0.230$ V *vs* NHE is obtained. At pH ≤ 5, the couple was chemically irreversible because of the rapid hydrolysis/isomerization,[11] and so E_{pc} is plotted. The voltage scan was normally limited to the 0.0 to –0.7 V vs SCE range, but when the range was extended cathodic to + 300 mV, the growth of the pyridyl isomer at the expense of the amido complex was evident in multiple scans. In Figure 5, the dashed lines are imposed for $E_{pc}((NH_3)_5Ru(NHC(O)\text{-}4\text{-}py^{3+/2+})) = -500$ mV vs SCE with the following pK_a values: A, 6.2 for $(NH_3)_5Ru^{II}(NHC(OH)\text{-}4\text{-}py)^{2+}$; B, pK_a = 4.3 for $(NH_3)_5Ru^{III}(NHC(O)\text{-}4\text{-}pyH)^{3+}$; C, 3.5 for $(NH_3)_5Ru^{II}(NHC(OH)\text{-}4\text{-}pyH)^{3+}$ (from the pH dependence of the isomerization yields[11]). The pH 2–6 data do not require the fit shown but are consistent with it.

Our observations on the (carboxamido)ruthenium(III) complexes are generally in agreement with those of earlier workers.[7] Thus we also find no evidence for protonation of the amido function in the pyridyl derivatives above pH 1. However, in contrast to an earlier report,[7] pH-independent $E_{1/2}$ values are observed only above pH 8 for the benzamido complex and above pH 4–7 for the pyridyl derivatives.

Spectral and electrochemical results for carboxamide complexes are summarized in Tables 3 and 4 in which relevant comparisons from the literature are also included.

The solvent dependence of the spectrum of the benzamide complex $(NH_3)_5Ru^{III}(NHC(O)Ph)^{2+}$ was examined (solvent, donor number, λ_{max} in nm): nitromethane, 2.7, 412; acetonitrile, 14.1, (318) 408; H_2O, (18), (314) 390; DMF, 26.6, (320) 398; DMSO, 29.8, (320) 396. The solvent dependence of the spectrum of $Ru(NH_3)_5Cl^{2+}$ is as follows: nitromethane, 2.7, 376; acetonitrile, 14.1, 344; acetone, 17, 342; H_2O, (18), 327; DMF, 26.6, 336; DMSO, 29.8, 334.

Carboxamido–Ru(II) Complexes. From the electrochemical behavior of the carboxamido complexes and the stopped-flow studies reported earlier,[11] it was expected that the Ru(II) complexes would be unstable in water and undergo relatively rapid aquation. Thus we attempted to observe the spectra of the $(NH_3)_5Ru^{II}(NHC(O)R)$ complexes produced as intermediates in electron-transfer reactions. Because the aquation rates of the protonated species are greater than those of their conjugate bases, the experiments were conducted at pH ≥7.

The reduction of $(NH_3)_5Ru^{III}(NHC(O)\text{-}4\text{-}py\text{-}N\text{-}Me)^{3+}$ was examined in 0.05 M NaAc (final pH 5.8). With V(II) as reductant, a transient blue color was produced in the solution. As is shown in Figure 6, the 695-nm absorption band decayed with a half-life of ca. 30 s at 5 °C. No color resulted when V(II) was mixed with the free ligand under the same conditions. With aquachromium(II) as reductant, λ_{max} of the transient (possibly an RuNHC(O–Cr) species resulting from inner-sphere electron transfer[27]) was at 650 nm. In aged product solutions containing V(II), a species with λ_{max} = 380 and 630 nm formed over several hours. It was also formed from V(II) and $(NH_3)_5Ru(OH_2)^{2+}$ under the same conditions and is a Ru–O–V complex already described in the literature.[28]

Analogous experiments were conducted with the other complexes. For experiments at pH >5, sodium dithionite was used as reducing agent instead of V(II). Typically, solutions 0.5 mM in the $Ru^{III}(NHC(O)R)$ complex, dissolved in 0.01 M buffer, were reduced with 2 mM $Na_2S_2O_4$. Dithionite concentrations were chosen so that the electron-transfer step would be much more rapid than the loss of the amide ligand. The resulting spectra are shown in Figure 7. A few runs in which the rate law for the electron-transfer step was investigated indicated that the kinetics are complex, involving both[29] the SO_2^- radical and its $S_2O_4^{2-}$ parent as kinetically significant reductants.

In order to verify that the blue transient produced from V(II) and $(NH_3)_5Ru^{III}(NHC(O)\text{-}4\text{-}py\text{-}N\text{-}Me)^{3+}$ was the corresponding

(26) Fasman, G. D., Ed. *Handbook of Biochemistry and Molecular Biology*, 3rd ed.; CRC Press: Boca Raton, FL, 1976; Vol. 1, p 338.
(27) Stritar, J. A.; Taube, H. *Inorg. Chem.* **1969**, *8*, 2281–2292.
(28) De Smedt, H.; Persoons, A.; De Maeyer, L. *Inorg. Chem.* **1974**, *13*, 90–96.
(29) Creutz, C.; Sutin, N. *Inorg. Chem.* **1974**, *13*, 2041–2043.

Table 3. Redox Potentials and pK Values for Carboxamido Ruthenium Complexes $(NH_3)_5Ru(NHC(O)R)^a$

R	$E_{1/2}^{am,H}$, V *vs* NHE	$E_{1/2}^{am}$, V *vs* NHE	$pK_{a,amH^{II}}$	$pK_{a,amH^{III}}$
Ph	+0.13	–0.25	8.0 ± 0.3	0.9[b]
4-pyCH_3	>+0.08 (+0.13 calcd)	–0.13	4.2 ● 0.3	(–0.3)
4-py$Ru^{II}(NH_3)_5$	≥+0.17[c]	–0.15	4.3 ± 0.3	<0.6
4-py[d]		–0.23	6.2 ± 0.5	
CH_3				2.0[b]
CH_2NH_2[e]		–0.265	4.3 ± 0.2	ca. –1
(*N*-Et)CH_2NH_2[e]		–0.230	5.1 ± 0.2	ca. –1
(*N*-CH_2CO_2)CH_2NH_2[e]		–0.265	5.2 ± 0.2	ca. –1

[a] Data from this study in 0.1 M KCF_3SO_3 unless otherwise noted. [b] Zanella, A. W.; Ford, P. C. *Inorg. Chem.* **1975**, *14*, 42–47. [c] Chou, M. H.; Creutz, C.; Sutin, N. *Inorg. Chem.* **1992**, *31*, 2318–2327. [d] From the pH dependence of the UV spectrum in 0.5 M KCF_3SO_3, the pK of the Ru(III)pyridyl group is 4.3 ± 0.3. [e] Ilan, Y.; Taube, H. *Inorg. Chem.* **1983**, *22*, 1655–1664. These amides are chelated to the *cis*-$Ru(NH_3)_4$ fragment through the amine and amido nitrogens.

Table 4. Electronic Absorption Spectra of $(NH_3)_5Ru^{III}(NHC(O)R)$ Complexes and their Conjugate Acids[a] in Aqueous Solutions at Room Temperature

	λ_{max}, nm (ϵ, M^{-1} cm^{-1})	
R	$Ru^{III}NHC(O)R$	$Ru^{III}NHC(OH)R$
Ph[b]	393 (4.1×10^3)[c]	385 (1.5×10^3)[c]
	314 (3.7×10^3)	320 (3.5×10^3)
	270 (2.7×10^3)	270 (3.8×10^3)
	219 (9.5×10^3)	228 (9.4×10^3)
4-py	386 (3.2×10^3)[d]	
	306 (3.1×10^3)	
	270 (3.7×10^3)	
4-pyH	358 (4.7×10^3)[e]	
	264 (4.7×10^3)	
4-(N-Me)py	358 (5.0×10^3)[d]	315 (4.7×10^3)[f]
	268 (4.7×10^3)	274 (6.3×10^3)
	220 (7.2×10^3)	220 (7.2×10^3)
4-py$Ru^{III}(NH_3)_5$	348 (5.2×10^3)[g]	310 (4.7×10^3)[g]
	272 (5.7×10^3)	280 (9×10^3)
CH_3	383 (3.5×10^3)[c]	322 (1.6×10^3)[c]
	249 (2.3×10^3)	
3-py	387 (3.7×10^3)[h]	
3-pyH	359 (2.9×10^3)[h]	

[a] Data from this study in 0.1 *M* KCF_3SO_3 unless otherwise noted. [b] In pH 8, 0.02 M phosphate buffer, the free benzamide spectrum is as follows (λ_{max}, nm (ϵ, M^{-1} cm^{-1})): 268 (sh 674), 226 (8.8×10^3), 202 (7.5×10^3). [c] Zanella, A. W.; Ford, P. C. *Inorg. Chem.* **1975**, *14*, 42–47. [d] In aqueous pH 6.8 phosphate buffer. [e] In 0.1 M triflic acid. [f] In 9.0 M triflic acid; in 9.0 M perchloric acid, the peaks were shifted to about 5 nm longer wavelength. [g] Chou, M. H.; Creutz, C.; Sutin, N. *Inorg. Chem.* **1992**, *31*, 2318–2327. [h] Huang, H.-Y.; Chen, W.-J.; Yang, C.-C.; Yeh, A. *Inorg. Chem.* **1991**, *30*, 1862–1868.

Ru(II) complex, the pyridyl-alkylated ligand $(NH_2C(O)$-4-py-*N*-Me$)(CF_3SO_3)$ was prepared and combined with $(NH_3)_5Ru(OH_2)^{2+}$ in alkaline solution. A 690-nm absorbing species was indeed observed to grow in (see Figure 6, bottom). The formation rate increased with ligand (0.01–0.06 M), and the yield increased with both amide and hydroxide ion (0.01–0.02 M) concentrations, as is predicted for eq 2c. In the first experiments, the data were

$$(NH_3)_5Ru(OH_2)^{2+} + NH_2C(O)R = (NH_3)_5Ru^{II}(NHC(OH)R)^{2+} + H_2O \quad K_{amH^{II}} \quad (2a)$$

$$(NH_3)_5Ru^{II}(NHC(OH)R)^{2+} = (NH_3)_5Ru^{II}(NHC(O)R)^{+} + H^{+} \quad K_{a,amH^{II}} \quad (2b)$$

$$(NH_3)_5Ru(OH_2)^{2+} + NH_2C(O)R = (NH_3)_5Ru^{II}(NHC(O)R)^{+} + H^{+} \quad K_{amII} \quad (2c)$$

not very reproducible from day to day, the blue colors did not persist, and the pH values of the solutions dropped significantly. We eventually traced the origin of these problems to the hydrolysis of the free amide (eq 1) to give the free carboxylate (vide supra). (On the basis of results presented below, binding of the carboxylate

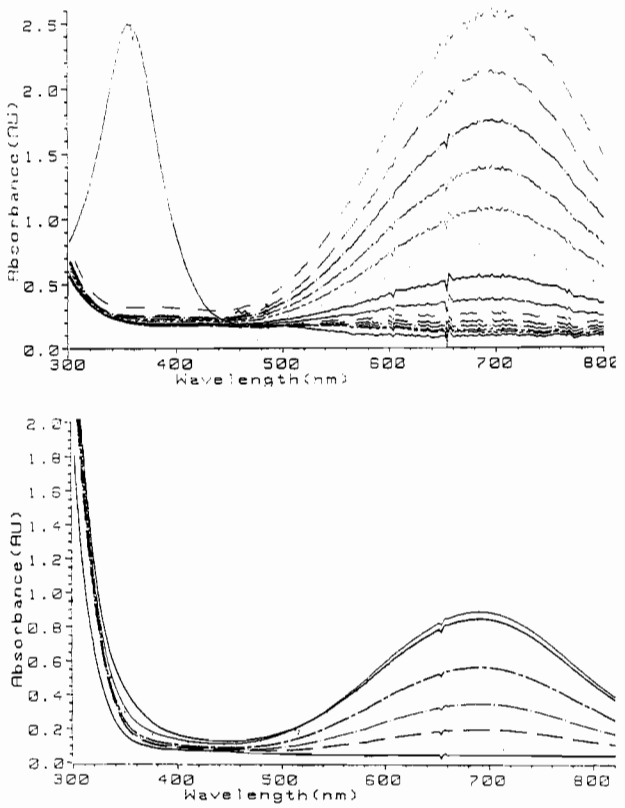

Figure 6. Spectra of $(NH_3)_5Ru^{II}(NHC(O)$py-*N*-Me$)^{2+}$. Top: A solution of 0.5 mM $(NH_3)_5Ru^{III}(NHC(O)$py-*N*-Me$)^{3+}$ dissolved in 0.05 M acetate buffer (final pH 5.8) is reduced with aquavanadium(II) (final 15 mM) at 5 °C (1-cm cell). The 360-nm peak is that of the Ru(III) complex prior to the addition of the V(II). The 695-nm peak is observed within 3 s of mixing and decreases in intensity with time. The scans shown are separated in time by 7 s. Bottom: Separately deaerated stock solutions of base, ligand, and Ru(II) are mixed to give a solution 0.01 M in NaOH, 0.01 M in $(NH_2C(O)$py-*N*-Me$)(CF_3SO_3)$, and 0.5 mM in $(NH_3)_5Ru(OH_2)^{2+}$ (1-cm cell) at 25 °C. The 690-nm absorption increases with time over about an hour and then disappears slowly. Scans shown for t = 1, 5, 10, 20, 30, and 45 min.

product to Ru(II) does not occur to a significant extent under these conditions.) Under the conditions used, amide hydrolysis occurs on approximately the same time scale as substitution of Ru(II) on the amide. Since the amide hydrolysis had not been anticipated, mixtures of the amide in NaOH had been prepared and deaerated for varying lengths of time before use. Thus the irreproducibility of the results arose from varying degrees of amide and hydroxide ion consumption having taken place prior to the Ru(II) addition. In the experiment illustrated in Figure 6, all of the (deaerated) reagents were mixed just prior to the first scan. Thus the blue species ($\epsilon_{690} \geq 6.0 \times 10^3$ M^{-1} cm^{-1}) is $(NH_3)_5Ru^{II}(NHC(O)$-4-py-*N*-Me$)^{2+}$.

We also examined eq 2 with benzamide as ligand. (On the

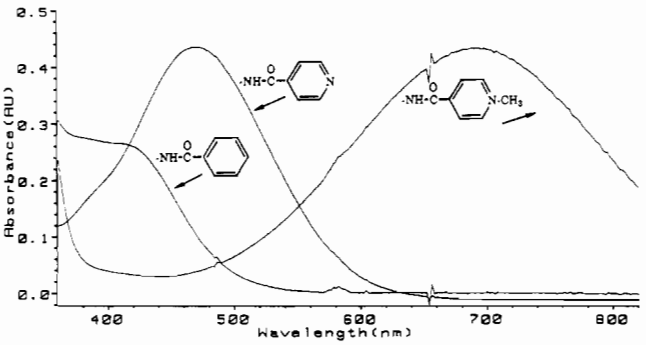

Figure 7. Spectra of carboxamido–Ru(II) complexes as a function of R at 25 °C and μ = 0.1 M ($CF_3SO_3^-$). Solutions 0.5 mM in the Ru^{III}-(NHC(O)R) complex, dissolved in pH 11, 0.01 M phosphate buffer, were reduced with 2 mM $Na_2S_2O_4$ with use of a handheld HiTech stopped flow device and scanned in a HP diode array spectrometer. The spectra shown were obtained within 0.5 s of mixing.

time scale of these experiments, hydrolysis of benzamide is not a complication.[20]) A broad absorption with "peaks" at 390 and 410 nm grew in after mixing the Ru(II) with benzamide in 0.01 M OH^-. After about 10 min, the band shape changed, with the short wavelength side growing in relative intensity to give a peak at 380 nm with a shoulder at about 410 nm. Also, as monitored at 380 nm, the reaction was biphasic: with a fit to two exponentials, 60–70% of the absorbance change occurred with a benzamide-dependent rate constant, $k_{obs,1} = (7 \pm 1) \times 10^{-2}$[benzamide] s^{-1}, while the residual absorbance increase occurred with $k_{obs,2} \sim 2.5 \times 10^{-4}$ s^{-1} at 25 °C and 0.01 M NaOH. With 0.01 M NaOH and (0.3–0.6) mM Ru(II), the yield of complex was the same with 0.05, 0.07, and 0.083 M benzamide, but only 66% and 87% as great with 0.01 and 0.02 M amide, suggesting an effective K ($=K_{am^{II}}/[H^+]$) value of ca. (200 ± 100) M^{-1} under these conditions. The maximum absorbances observed yield $\epsilon_{380} \geq 4.0 \times 10^3$ M^{-1} cm^{-1}. Upon standing overnight, the 380-nm absorptions disappeared and only a 340-nm shoulder remained; a brown precipitate was frequently evident in the cell. (The chemistry responsible for this decomposition is not known. Hydrolysis of the bound amide should produce $Ru(NH_3)_6^{2+}$ and benzoate, but the observed products are not consistent with simple amide hydrolysis. Possibly the source of the decomposition is disproportionation, for example to RuO_2 and ruthenium metal, or oxidation by water, to give RuO_2 and H_2.)

A few experiments were performed with $NH_2C(O)$-3-py-*N*-Me^+ as ligand (L). The formation of the complex was monitored at its 472-nm maximum ($\epsilon \geq 2.5 \times 10^3$ M^{-1} cm^{-1}) at 25 °C, μ = 0.1 M ($LiCF_3SO_3$). In the presence of 0.01 M OH^-, a pseudo-first-order dependence on $[(NH_3)_5RuOH_2^{2+}]$ (initially 0.5 mM) was obtained and k_{obsd} values of 1.9×10^{-4} s^{-1} (0.01 M L), 4.6×10^{-4} s^{-1} (0.02 M L) and 8.6×10^{-4} s^{-1} (0.05 M L) were found. The same second-order rate constant ($k_{obsd}/[L] = 2.1 \times 10^{-2}$ M^{-1} s^{-1}) was obtained in a pH 9 borate buffer.

From the yields of $(NH_3)_5Ru^{II}(NHC(O)R)^{2+}$ obtained in pH 6.8 phosphate buffer in the presence of 0.05 M amide, $K_{amH^{II}}$ values (eq 2a) of 1×10^{-7} and 5×10^{-8} are estimated for R = 4-py-*N*-Me^+ and R = 3-py-*N*-Me^+, respectively.

Earlier[11] we studied the aquation (k_{off}) of amido complexes at 25.0 °C, 0.1 M ionic strength ($LiCF_3SO_3$). Here we have obtained estimates of the rate constants (k_{on}) for substitution of the amides on $(NH_3)_5RuOH_2^{2+}$ and of equilibrium quotients for the amido complexes at pH ≥7. For R = 4-py-*N*-Me^+ and 3-py-*N*-Me^+, lower limits to k_{on} are derived from apparent values (1×10^{-2} and 2.1×10^{-2} M^{-1} s^{-1}, respectively) obtained for solutions (0.01 M OH^-, 0.01–0.05 M ligand, μ = 0.1 M, 25 °C) later recognized to be undergoing parallel amide hydrolysis. An upper limit of 10^{-1} M^{-1} s^{-1} is suggested by the behavior of other systems.[30] The kinetic and equilibrium data are summarized in Table 5, along with spectral data for the Ru(II) complexes.

A Carboxylato–Ruthenium(II) Complex. The properties of $(NH_3)_5Ru^{II}(O\text{–}C(O)R)^+$, R = 4-py-*N*-$Me^+$, were partially characterized for comparison with the analogous carboxamido complexes and the mixed-valence complex[10] containing the bridging isonicotinate ligand. No evidence for formation of the complex was detected on mixing $(NH_3)_5RuOH_2^{2+}$ (0.5 mM) with ≤0.05 M O–C(O)-4-py-*N*-Me. However, a faint blue hue was produced when the Ru(II) concentration was increased 10-fold in a deaerated pH 5 solution containing 0.1 M $Na(CF_3SO_3)$ at 25 °C: $A_{600} = 0.18 \pm 0.03$, 0.05 M L; $A_{600} = 0.45 \pm 0.01$, 0.1 M L (three determinations each). The blue color of the Ru(II) complex was also evident in the solution (1.7 M L) used to prepare the Ru(III) complex (see Experimental Section). The Ru(III) complex exhibited a reversible cyclic voltammogram at pH 4–9, with $E_{1/2}$ = –0.053 V vs NHE at 22 ± 2 °C, 0.1 M $Na(CF_3SO_3)$, and a sweep rate of 100 mV/s. The visible spectrum of the Ru(II) complex and its aquation rate were determined by reducing 0.5 mM $(NH_3)_5Ru^{III}(O\text{–}C(O)R)^{2+}$ solutions with 5 mM $Na_2S_2O_4$ (final concentrations) in a hand-driven stopped-flow at pH 5, 7, or 9 (10 mM acetate, phosphate, or borate) and monitoring the spectrum in an HP diode array spectrometer. A broad absorption with λ_{max} = 605 ± 5 nm formed in all of the solutions and disappeared with a rate constant of 1.1 ± 0.1 s^{-1} at 25 °C (0.6 s^{-1} for one measurement at 15 °C); the extrapolated initial absorbance value was 0.7 ± 0.1 at 600 nm with 1-cm pathlength. Assuming 100% yield of $(NH_3)_5Ru^{II}(O\text{–}C(O)R)^+$ at zero time, $\epsilon_{600} = 1.4 \times 10^3$ M^{-1} cm^{-1}. On the basis of this molar absorptivity and the magnitudes of the 600-nm absorbances reported above for incomplete formation of $(NH_3)_5Ru^{II}(O\text{–}C(O)R)^+$, the equilibrium constant for eq 3, R = 4-py-*N*-Me^+, is 0.58 ± 0.1 M^{-1} at 25 °C. From the product of this equilibrium constant and the

$$(NH_3)_5Ru(OH_2)^{2+} + {}^-OC(O)R = (NH_3)_5Ru^{II}(OC(O)R)^+ + H_2O \quad (3)$$

aquation rate constant (k_{off}), the rate constant for the substitution eq 3 is 0.6 M^{-1} s^{-1} at 25 °C.

The cyclic voltammetry of *N*-methylated isonicotinamide and isonicotinate was carried out in acetonitrile. Both free ligands and complexes exhibited quasi-reversible cyclic voltammograms (ΔE_p 85–95 mV at 100–300 mV/s sweep rate) in CH_3CN at 22 ± 2 °C. The $E_{1/2}$ value of the ferrocenium/ferrocene couple was +393 mV vs SCE under these conditions. The free ligands O–C(O)R and $H_2N\text{–}C(O)R^+$, R = 4-py-*N*-Me^+, exhibited $E_{1/2}$ values of –1.30 and –0.91 V vs SCE, respectively. The complexes exhibited both metal- and ligand-centered reduction processes with $E_{1/2}$ values of –0.133 and –1.19 V vs SCE (O–C(O)R) and –0.300 and –1.23 V vs SCE (NH–C(O)R). In aqueous media only the cathodic portion of the ligand-centered reduction was observed for both the free and complexed ligands.

Kinetic, equilibrium, and spectral data for the carboxylate complex are compared with those of its parent amide in Table 6.

Discussion

Structural features of the complexes studied here are compared with relevant literature results in Table 7. The structure of the $(NH_3)_5Ru^{III}NHC(O)R$ complex is most closely related to that of the glycinamido–tetraammineruthenium(III)[9] complex in which the Ru–NRHC(O) bond length is 1.966(4) Å compared to 1.988(9) Å in the present structure. The Ru(III)–N amido bond distance is significantly shorter than the Ru(III)–NH_3 bonds in this complex and in hexaammineruthenium(III) (2.104(4) Å[31]); it is comparable to that (average 2.020(4) Å) found for the μ-NH_2

(30) Taube, H. *Comments Inorg. Chem.* **1981**, *1*, 17–31.

(31) Stynes, H. C.; Ibers, J. A. *Inorg. Chem.* **1971**, *10*, 2304–2308.

Table 5. Kinetic, Thermodynamic, and Spectral Data for $(NH_3)_5Ru^{II}(NHC(O)R)$ Complexes in Aqueous Media at Room Temperature

	Ph	4-py	4-py-*N*-Me$^+$	3-py-*N*-Me$^+$	4-py$Ru^{II}(NH_3)_5$[c]
$k_{on,amH^{II}}$, M^{-1} s^{-1}	$(7 \pm 1) \times 10^{-2}$		$\geq 1.2 \times 10^{-2}$	$\geq 2.1 \times 10^{-2}$	
$k_{off,amH^{II}}$,[a] s^{-1}	34	24	6		
k^{II}_{on}/k^{II}_{off}, M^{-1}	2.1×10^{-3}		$\geq 2 \times 10^{-3}$		
$pK_{a,amH^{II}}$	7.7	6.2	4.2		4.3
$K_{am^{II}}$	$\sim 2 \times 10^{-10}$		1×10^{-7}	5×10^{-8}	1×10^{-7}
$K_{am^{II}}/K_{a,amH^{II}}$, M^{-1}	1×10^{-2}		1.7×10^{-3}		2×10^{-3}
$K_{am^{III}}/K_{am^{II}}$ [b]	2×10^5	1×10^5	2×10^3		5×10^3
$K_{am^{III}}$	4×10^{-5}		2×10^{-4}		6×10^{-4}
$K_{amH^{III}}$, M^{-1}	4×10^{-6}		4×10^{-5}		1×10^{-4}
λ_{max}, nm	380	475	695	472	
ϵ, M^{-1} cm^{-1}	4×10^3	7×10^3	6.9×10^3	2.5×10^3	

[a] Chou, M. H.; Brunschwig, B. S.; Creutz, C.; Sutin, N.; Yeh, A.; Chang, R. C.; Lin, C.-T. *Inorg. Chem.* **1992**, *31*, 5347–5348. [b] The $K_{am^{III}}/K_{am^{II}}$ values are obtained from the difference in reduction potentials for the amide and aqua couples, $E_{1/2}((NH_3)_5Ru(OH_2)^{3+/2+}) = +0.067$ V vs. NHE (Matsubara, T.; Ford, P. C. *Inorg. Chem.* **1976**, *15*, 1107–1110). [c] From Chou, M. H.; Creutz, C.; Sutin, N. *Inorg. Chem.* **1992**, *31*, 2318–2327.

Table 6. Comparison of $(NH_3)_5Ru^{II}(NHC(O)R)$ and $(NH_3)_5Ru^{II}(OC(O)R)$ Complexes in Aqueous Solution at Room Temperature

	–OC(O)-4-py-*N*-Me	–NHC(O)-4-py-*N*-Me$^+$
λ_{max}, nm (ϵ, M^{-1} cm^{-1})	600 ($1.4 \pm 0.2 \times 10^3$)	695 (6.9×10^3)
free *L*: $E_{1/2}(L^{0/-})$, V	–1.30[a]	–0.91[a]
complex: $E_{1/2}(Ru^{III/II})$, V	–0.133[a]	–0.300[a]
$E_{1/2}(L^{0/-})$, V	–1.19[a]	–1.23[a]
$E_{1/2}(Ru^{III/II})$, V vs NHE	–0.053[b]	–0.13[b]
k_{off}^{II}, s^{-1}	1.1 ± 0.1[c]	$\leq 2 \times 10^{-3}$ [d] (10^{-6})[e]
k_{on}^{II}, M^{-1} s^{-1}	0.6[f]	(10^1)[e]
$K_{L\text{-}II}$, M^{-1}	0.58 ± 0.1 (eq 3)	10^6–10^8 (eq 2d)
$K_{L\text{-}III}$, M^{-1}	55	10^9–10^{11}

[a] In acetonitrile containing 0.1 M TBAH, V vs SCE. [b] In 0.5 M $Na(CF_3SO_3)$ at pH 4–9. [c] In 0.1 M $Na(CF_3SO_3)$ at pH 4–9. [d] Chou, M. H.; Brunschwig, B. S.; Creutz, C.; Sutin, N.; Yeh, A.; Chang, R. C.; Lin, C.-T. *Inorg. Chem.* **1992**, *31*, 5347–5348. [e] Calculated from k_{on}^{II} and $K_{L\text{-}II}$, assuming $k_{on}^{II} = 10^1$ M^{-1} s^{-1} and $K_{L\text{-}II} = 10^6$ M^{-1}. [f] Calculated from the product of k_{off}^{II} and $K_{L\text{-}II}$.

bridges in "ruthenium black".[32] (However, in the latter, the highly acute Ru–N–Ru angle, 81.0(1)°, suggests a Ru–Ru bonding interaction.) It is also comparable to that (1.980(12) Å) of the "nitrile" bound cyanamide ligand in $(NH_3)_5Ru(2,3\text{-}Cl_2pycd)^{2+}$ (2,3-Cl_2pycd = 2,3-dichlorophenylcyanamide anion).[33] The very short Ru–N distance in the amido complex is due to π-electron donation from the sp^2-hybridized N lone pair to the half-occupied πd Ru(III) orbital. (The Ru–N(1)–C(1) angle (126.3 (8)°) is consistent with sp^2 rather than sp^3 hybridization at nitrogen in the complex.) Consistent with the powerful donor nature of this ligand toward Ru(III) is the observation[7] that the ammonia symmetric deformation frequencies of amidoruthenium(III) are shifted to lower frequencies (1297–1310 cm^{-1}) than the range of 1330–1360 cm^{-1} expected for ruthenium(III) ammine complexes.

The electronic structures of amides are generally discussed in terms of resonance structures **I** and **II**; for N-bonded metal amide complexes of M^+, the analogues are **IM** and **IIM**. Structure **IIIM** incorporates πp–πd electron donation:

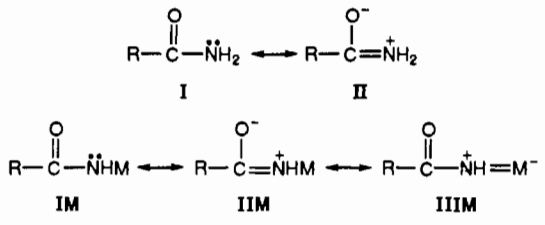

There is no evidence that resonance structure **IIM** is important for the Ru(III) complexes. The C—N and C=O bond lengths in the coordinated amide groups of both the chelated glycinamido and the present carboxamide Ru(III) complexes are identical within error with those in the free amide groups of the pyridyl-bonded isonicotinamide complexes. As discussed by Ilan and Kapon,[9] this is consistent with the short Ru(III)–amido bond (resonance structure **IIIM**). Such behavior is in striking contrast to that found when metal πd holes, which facilitate N-πp M-πd multiple bonding, are absent; thus for Co(III) and the analogous metal centers (including, presumably Ru(II)), the M—N bonds are not as greatly shortened (compared to M—NH_3) and the C=O and C—N bonds are longer and shorter, respectively, than in the free amides and in the Ru(III) complexes, indicating that the resonance structure **IIM** is important in these complexes. A notable difference between the present structure and those of the three pyridyl-bonded isonicotinamide complexes in Table 7 is in the planarity of NHRuC(O)– and the pyridyl part of the ligand. For the amido-bonded species, the two groups are coplanar, while in the others, the $NH_2C(O)$– is rotated 10 to 34° from the plane of the pyridine ring.

The reduction potentials of the amido complexes (Table 3) are rather negative, –0.13 to –0.25 V *vs* NHE. By contrast, the reduction potentials of the protonated carboxamide complexes, *ca.* +0.1 to +0.2 V *vs* NHE are slightly higher than those of $(NH_3)_5RuH_2O^{3+/2+}$ and $Ru(NH_3)_6^{3+/2+}$, +0.067 and +0.05 V *vs* NHE,[34] respectively. We have argued that the site of protonation is the oxygen of the carboxamide ligand in these complexes.[10] The acidities of the protonated Ru(III) carboxamide complexes lie in the same region as those reported for uncomplexed amides[26,35] and are 5–7 orders of magnitude greater than those of the corresponding Ru(II) complexes. The pK's for Ru(II) carboxamide complexes are 4–8. This is consistent with an increased importance of resonance structure **II** for the Ru(II) complexes; through such resonance, Ru(II) πd electron density can be delocalized onto the carbonyl oxygen, making it more basic. The acidities of Pt(II) (imidol) amides $pK_a \sim 4$,[4] lie at the lower end of the region found for their Ru(II) counterparts.

Ligand Binding Equilibria. Table 5 summarizes kinetic and thermodynamic data obtained for carboxamido–ruthenium(II) complexes. (Values in the last column were obtained in earlier work.[10]) For R = Ph and 4-py-*N*-Me$^+$, there are two independent sources of information on the magnitude of $K_{amH^{II}}$: One value is derived from the kinetics (k_{on}/k_{off} for eq 2a), and the other is based on the equilibrium yield of the amido complex at known ligand and hydrogen ion concentrations ($K_{am^{II}}/K_{a,amH^{II}}$). Since there were difficulties with both the k_{on} and $K_{am^{II}}$ measurements because of the side reactions occuring in alkaline media, the errors are expected to be large, but probably not greater than a factor of 10.

As noted earlier,[10] the site of protonation in the protonated carboxamide complexes is believed to be the amide oxygen. Consequently the thermodynamics of eq 4 should be considered

(32) Flood, M. T.; Ziolo, R. F.; Earley, J. E.; Gray, H. B. *Inorg. Chem.* **1973**, *12*, 2153–2156.
(33) Crutchley, R. J.; McCaw, K.; Lee, F. L.; Gabe, E. J. *Inorg. Chem.* **1990**, *29*, 2576–2581.
(34) Matsubara, T.; Ford, P. C. *Inorg. Chem.* **1976**, *15*, 1107–1110.
(35) Yates, K.; Riordan, J. C. *Can. J. Chem.* **1965**, *43*, 2328–2335.

Table 7. Comparisons of $(NH_3)_5Ru^{III}(NHC(O)\text{-}4\text{-}py\text{-}N\text{-}Me)^{3+}$ and $(NH_3)_5Ru^{II}(py\text{-}4\text{-}C(O)NH_2)^{2+}$ with other Structures

Ruthenium Coordination Sphere

complex	d(Ru–N_R), Å	d(Ru–NH_3), Å
$(NH_3)_5Ru^{III}(NHC(O)4\text{-}py\text{-}N\text{-}Me)^{3+}$ [a]	1.998(9)	2.121(8)
$(NH_3)_4Ru^{III}(NH_2CH_2C(O)NH)^{2+}$ [b]	1.966(4)	2.130(5)
$(NH_3)_4Ru^{III}(NH_2)_2Ru^{III}(NH_3)_4^{4+}$ [c]	2.020(4) av	2.173(3)
$Ru^{III}(NH_3)_6^{3+}$ [d]		2.104(4)
$(NH_3)_5Ru^{II}(py\text{-}4\text{-}C(O)NH_2)^{2+}$ [a]	2.049(7)	2.136(8) av
$(NH_3)_5Ru^{II}(pz)^{2+}$ [e]	2.006(6)	2.155(6) av
$(NH_3)_5Ru^{II}(pz\text{–}Me)^{3+}$ [f]	1.95(1)	2.129(8) cis; 2.122 (7) trans
$(NH_3)_4Ru^{II}(py\text{-}4\text{-}C(O)NH_2)_2^{2+}$ [g]	2.058(6)	2.155(11)
$Ru^{II}(NH_3)_6^{2+}$ [d]		2.144(4)
$(NH_3)_4Ru^{III}(py\text{-}4\text{-}C(O)NH_2)_2^{3+}$ [g]	2.099(4)	2.125(7)

Intraligand Features

complex	d(C(O)–N), Å	d(C=O), Å	d(C(O)–py), Å
$(NH_3)_5Ru^{III}(NHC(O)\text{-}4\text{-}py\text{-}N\text{-}Me)^{3+}$ [a]	1.325(15)	1.236(15)	1.508(16)
$(NH_3)_5Ru^{II}(py\text{-}4\text{-}C(O)NH_2)^{2+}$ [a]	1.322(12)	1.242(11)	1.512(12)
$(NH_3)_4Ru(py\text{-}4\text{-}C(O)NH_2)_2^{3+}$ [g]	1.332(8)	1.221(7)	1.509(8)
$(NH_3)_4Ru(py\text{-}4\text{-}C(O)NH_2)_2^{2+}$ [g]	1.329(53)	1.22(20)	1.508(37)
$(NH_3)_4Ru^{III}(NH_2CH_2C(O)NH)^{2+}$ [b]	1.334(6)	1.244(6)	

[a] This work. [b] The chelate *cis*-glycinamide. Ilan, Y.; Kapon, M. *Inorg. Chem.* **1986**, *25*, 2350–2354. [c] Flood, M. T.; Ziolo, R. F.; Earley, J. E.; Gray, H. B. *Inorg. Chem.* **1973**, *12*, 2153–2156. [d] Stynes, H. C.; Ibers, J. A. *Inorg. Chem.* **1971**, *10*, 2304–2308. [e] Gress, M. E.; Creutz, C.; Quicksall, C. O. *Inorg. Chem.* **1981**, *20*, 1522–1528. [f] Wishart, J. F.; Bino, A.; Taube, H. *Inorg. Chem.* **1986**, *25*, 3318–3321. [g] These are *cis*-bis(isonicotinamide) complexes in which the isonicotinamide ligands are attached to ruthenium through the pyridyl nitrogen. Richardson, D. E.; Walker, D. E.; Sutton, J. E.; Hodgson, K. O.; Taube, H. *Inorg. Chem.* **1979**, *18*, 2216–2221.

in interpreting the data in Table 6. Unfortunately data for eq 4

$$NH_2C(O)R \rightleftharpoons NH{=}C(OH)R \qquad (4a)$$

$$NH{=}C(OH)R \rightleftharpoons NH{=}C(O^-)R + H^+ \qquad (4b)$$

are not available. The magnitude of $K_{amH^{II}}$ (eq 2a) is similar for the three pyridyl-containing complexes for which estimates are available. However, $K_{am^{II}}$ is considerably smaller for R = Ph because of the lower value of its $K_{a,amH^{II}}$ (Scheme 1). The electrochemical results indicate that the deprotonated carboxamide ligand stabilizes Ru(III) significantly more than Ru(II), consistent with the great basicity of the nitrogen, the short Ru(III)–N distance (Table 6), and the high ligand-field strength reported for the cobalt complexes.[36] This differential stabilization diminishes in the order Ph ~ 4-py > 4-py-*N*-Me$^+$, suggesting that electron-withdrawing groups attenuate the basicity of the nitrogen "lone pair". The values $K_{am^{III}} \sim 10^{-5}$ (R = Ph) and $\sim 10^{-4}$ (R = 4-py-*N*-Me$^+$) are obtained from the K^{III}/K^{II} ratios of 10^3–10^5. Differential stabilization of Ru(III) of this magnitude is greater than for H_2O (defined as 1), CH_3NH_2 (1),[37] Cl^- (2.5), NH_3 (5), or RCO_2^- ($\sim 10^2$), but significantly less than that for OH^- (10^9).[15]

The K_{amH} values should be related to the basicity of the amide nitrogen lone pair and to the stability of the COH tautomer (eq 4a). The K_{am} values are affected by the acidity of the amide—they reflect the ability of the metal to *replace* a proton on the free amide. The acidities of the free amides (eq 4a + eq 4b) should increase in the order Ph < 4-py < 4-py-*N*-Me$^+$. Taking the pK_a of free benzamide as 15,[10,38] the equilibrium constants for eq 2d are 10^5 and 10^{10} M^{-1} for Ru(II) and Ru(III), respectively, with R = Ph. For R = 4-py-*N*-Me$^+$, the pK_a of the free amide must

$$(NH_3)_5Ru(OH_2)^{2+} + NHC(O)R^- = (NH_3)_5Ru^{II}(NHC(O)R)^+ + H_2O \qquad (2d)$$

be less than that of benzamide and greater than ~12.5; assuming it is 14 ± 1, then the equilibrium constants for eq 2d are 10^6–10^8 M^{-1} and 10^9–10^{11} M^{-1} for Ru(II) and Ru(III), respectively. Thus although both Ru(II) and Ru(III) have a high affinity for *deprotonated* carboxamide, neither oxidation state competes very effectively with the proton for the very basic nitrogen in the carboxamido anion. Data for related systems are sparse: For acetamide and Pt(dien)$(H_2O)^{2+}$ in *acetone* solvent, values of K_{amH} (eq 2a) for both oxygen- and nitrogen-bonded (imidol) acetamide complexes have been determined to be 7 and 30, respectively.[4] Allowing for concentration (but not solvent) effects on the equilibrium, these correspond to 0.1 and 0.6 M^{-1}, respectively in water. The stability constant of an O-bonded macrocyclic cobalt(III) complex has been reported[3] to be 0.4 M^{-1} in water. Although the O-bonded acetamide complexes are reported to be the more stable form for $(NH_3)_5Ru^{II}$ and $(NH_3)_5Ru^{III}$,[4] there is no evidence for the O-bonded isomers with the aromatic amides studied here and previously.[10]

The affinities of both $(NH_3)_5Ru^{II}$ (eq 3) and $(NH_3)_5Ru^{III}$ for the OC(O)-4-py-*N*-Me carboxylate ligand (Table 6) are small—0.58 and 55 M^{-1}, respectively. This is consistent with the low basicity of the carboxylate oxygen: the pK_a of Hpy4-CO_2H^+ (protonated isonicotinic acid) is 1.99.[26] For R = CF_3 (pK_a 3.18), K^{III} = 300 M^{-1} at 60 °C.[39] From $E_{1/2}$ = –0.03 V *vs* NHE at 25 °C,[40] K^{II} = 6.9 M^{-1} for R = CF_3, assuming that K^{III} is independent of temperature. Although binding constants for OC(O)-4-py-*N*-Me are greater than those for the neutral amide, because of the pH dependence of eq 2d, the effective binding constants for the amide increase with pH; amide binding (eq 2a) is favored over carboxylate bonding (eq 3) at pH ≥1.5 for Ru(II) and at pH ≥6 for Ru(III).

Kinetics of Binding to Ru(II). Both the aquation rate constants and pK_a's of the Ru(II) amides decrease as the π-acceptor ability of the R group attached to the amide increases. However, the entire range of k_{off} values (6–35 s^{-1}) is only about 1 order of magnitude, in contrast to the wide p$K_{a,amH^{II}}$ variation, which is responsible for most of the observed difference in reactivity with respect to aquation. The k_{off} value for the carboxylate lies in the range (1–5 s^{-1}) reported by Stritar and Taube.[27]

Taube has pointed out that k_f values for the formation of $(NH_3)_5Ru^{II}L$ complexes span only the narrow range 10^{-2}–10 M^{-1}

(36) Fairlie, D. I. P.; Angus, P. M.; Fenn, M. D.; Jackson, W. G. *Inorg. Chem.* **1991**, *30*, 1564–1569.
(37) Yeh, A.; Taube, H. *Inorg. Chem.* **1980**, *19*, 3740–3742.
(38) Bordwell, F. G.; Ji, G.-Z. *J. Am. Chem. Soc.* **1991**, *113*, 8398–8401.
(39) Ohyoshi, A.; Shida, S.; Izuchi, S.; Kitigawa, F.; Ohkubo, K. *Bull. Chem. Soc. Jpn.* **1973**, *46*, 2431–2434.
(40) Ohyoshi, A.; Yoshikuni, K. *Bull. Chem. Soc. Jpn.* **1979**, *52*, 3105–3106.

Scheme 4

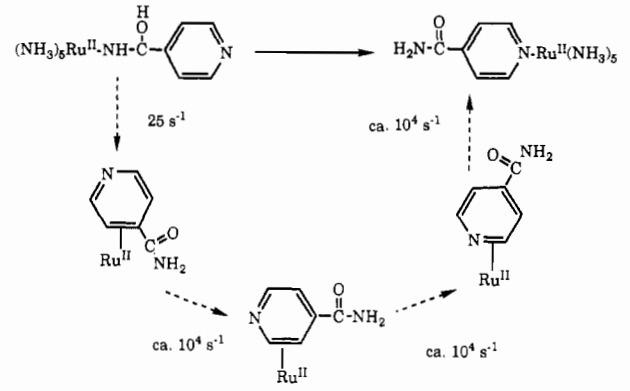

s^{-1} in a series in which the equilibrium constant varies from $> \sim 10^9$ M^{-1} to ~ 1 M^{-1}.[30] The observations presented here extend this pattern to a binding constant of $\sim 10^{-3}$ M^{-1}. In the series $(NH_3)_5RuL^{2+}$, the binding thermodynamics is almost exclusively reflected in the dissociation rate constant—$< 10^{-10}$ s^{-1} (isonicotinamide) to 30 s^{-1} (benzamide).

Earlier we reported evidence for π-bonded species in the isomerization of amide-bonded Ru(II) to pyridyl-bonded Ru(II) with R = 4-py and 3-py.[11] We neglected to consider the photochemical work of Durante and Ford,[41] which also provides evidence for such species, as well as a more direct evaluation of their reactivity. The photo-generated π-bonded (η^2) pyridine and 3-chloropyridine complexes (presumably 1,2-isomers) were found to revert to the stable *N*-pyridyl bonded species in high ($\sim$75%) yields with rate constants of ca. 10^4 s^{-1}. The pH dependence of yields and transient decay rates led to the inference of pyridyl pK_a values for π-bonded intermediates (**I**) lower than those for the free ligand (pK for pyridine 5.3, for **I** 3.8; with 3-chloropyridine 2.8 (free), 2.3 (**I**)). Folding this information into the mechanism for the thermal isomerization induced by protonation of the bound amide function,[11] a more detailed picture emerges (Scheme 4). In Scheme 4, formation of hydrolysis products, $(NH_3)_5Ru(OH_2)^{2+} + RC(O)NH_2$, could be a result of a 20–25% loss at each of the steps in the ring walk. In addition, the pK_a value of 3.3 suggested by the isomerization yield data may reflect the pK_a of the N-pyridyl protonated π-bonded (η^2) pyridine intermediates rather than that of $(NH_3)_5Ru^{II}NHC(OH)pyH^{3+}$. (In addition, in light of the intramolecular nature of O/N amide isomerization, π-bonded (η^2) species of the amide function[4] may also need to be considered.)

Spectra. Amidoruthenium(III) complexes exhibit bands in the 320–400-nm region (Table 4) attributable to ligand-to-metal charge transfer from the nitrogen lone pair of the deprotonated amido nitrogen to the vacant πd orbital of the Ru(III).[5,42] These bands have the same origin as that at 402 nm observed for deprotonated ruthenium hexaammine.[43,44] From the limited electrochemical data available for deprotonated amides, NH_2^-, +0.7 V,[45] acetamide, +0.73 V,[38] and benzamide, +0.82 V[38] *vs* NHE, the LMCT band energies do seem to increase as the oxidizability of the amide anion decreases. The similarities of the band maxima within the pairs $(NH_3)_5Ru(NHC(O)Ph)^{2+}$ (393 nm), $(NH_3)_5Ru(NHC(O)py)^{2+}$ (386 nm) and $(NH_3)_5Ru(NHC(O)4\text{-py-}N\text{-Me})^{3+}$ (358 nm), $(NH_3)_5Ru(NHC(O)4\text{-pyH})^{3+}$ (358 nm) are to be noted, as well as the shift between the two pairs.[46] Protonation or methylation of the pyridyl nitrogen clearly raises the energy of the amido nitrogen-to-Ru(III) charge-transfer band. In addition, the band energies qualitatively track the hydrolysis rates of their parent nitrile ruthenium(III) complexes:[5,7] R = $-CH_3 < -Ph < -py < -pyH^+/pyCH_3^+$. The trend in the hydrolysis rate constants has been attributed to the increasing electron-withdrawing power of the R, which activates the nitrile carbon toward nucleophilic attack. For the carboxamido complexes, increasing the electron-withdrawing power of R decreases the electron-donating ability of the nitrogen, rendering it more difficult to transfer electron density to Ru(III).

Table 8. LMCT Bands of L^+–Pentaammineruthenium(III) Complexes

compd	L	$E°(L/L^-)$,[a] V vs NHE	$E°(Ru^{III}/II)$, V vs NHE	λ_{max}, nm
1	I	1.33	(–0.03)[b]	541[c]
2	Br	1.92	–0.034	398[c]
3	Cl	2.41	–0.042	328[c]
4	NCSe	1.27	(+0.1)[d]	585[e]
5	NCS	1.63	+0.133[f]	495[e]
6	NCO	2.66	(+0.1)[d]	345[e]
7	pca 1[g]	0.84	–0.28	772
8	pca 17[g]	1.40	–0.036	645
9	HCO_2	2.0	+0.04[h]	294[h]
10	OH	1.90	–0.42[f]	298
11	CH_3CO_2	2.3	+0.09[h]	296[h]
12	$NHC(O)CH_3$	0.7[i]	–0.26[j]	383[k]
13	NHC(O)Ph	0.82[i]	–0.26	393[k]

[a] Stanbury, D. M. *Adv. Inorg. Chem.* **1989**, *33*, 69–137. [b] Assumed to be the same as for L = Br. [c] Verdonck, E.; Vanquickenborne, L. G. *Inorg. Chem.* **1974**, *13*, 762–764. [d] Assumed to be the same as for L = NCS. [e] Lin, S. W.; Schreiner, A. F. *Inorg. Chem. Acta* **1971**, *5*, 290–294. [f] Lim, H. S.; Barclay, D. J.; Anson, F. C. *Inorg. Chem.* **1972**, *11*, 1460–1466. [g] Substituted phenyldicyanamide ligand; see Table V in: Crutchley, R. J.; McCaw, K.; Lee, F. L.; Gabe, E. J. *Inorg. Chem.* **1990**, *29*, 2576–2581. [h] Ohyoshi, A.; Yoshikuni, K. *Bull. Chem. Soc. Jpn.* **1979**, *52*, 3105–3106. [i] Bordwell, F. G.; Ji, G.-Z. *J. Am. Chem. Soc.* **1991**, *113*, 8398–8401. [j] Assumed to be the same as for L = NHC(O)Ph. [k] Zanella, A. W.; Ford, P. C. *Inorg. Chem.* **1975**, *14*, 42–47.

The solvent dependence of the lower energy band of the benzamide complex is qualitatively consistent with the LMCT assignment although the magnitude of the sensitivity to solvent donor number is only $\sim$25% as great as reported for LMCT bands of pyridine-bound aminopyridine[47] and phenylcyanamide[33] complexes.

LMCT energies are expected to parallel the oxidizability of the ligand as reflected in its one-electron redox potential or ionization energy. It is interesting to test the LMCT assignment for the amido complexes by comparing the behavior of the LMCT spectra for the present complexes with those of other donor atoms, for example halides.[48] For low-spin d^5 Ru(III) or Os(III), LMCT is πX^- to t_{2g} (d_{xz}, d_{yz}) in character for the halides.[49] Data are collected in Table 8 and plotted in Figure 8. For the halides and pseudohalides in Table 8, E_{LMCT} tracks $E°(L/L^-)$ reasonably well with a slope of $\sim$1 and an intercept of $\sim$0.8 eV (the line shown is imposed, not fit). (This behavior may be compared with that of $Ru(NH_3)_6^{3+}|X^-$ ion pairs.[50] Values of $E_{LMCT} - \Delta E°$

(41) Durante, V. A.; Ford, P. C. *Inorg. Chem.* **1979**, *18*, 588–593.
(42) Fairlie, D. P.; Taube, H. *Inorg. Chem.* **1985**, *24*, 3199–3206.
(43) Waysbort, D.; Navon, G. *J. Chem. Soc., Chem. Commun.* **1971**, 1410–1411.
(44) Waysbort, D.; Evenor, M.; Navon, G. *Inorg. Chem.* **1975**, *14*, 514–519.
(45) Stanbury, D. M. *Adv. Inorg. Chem.* **1989**, *33*, 69–137.
(46) Despite the qualitative consistency of the behavior with the LMCT model, some anomalies remain for these complexes. One surprising aspect of the data in Table 4 is the contrasts in the spectra obtained on protonating the amido function in the benzamide complex (393 shifts to 385 nm) compared to the *N*-Me isonicotinamido (358 shifts to 315 nm) or acetamido complexes (383, 249 shifts to 322 nm[5]). Because of this striking difference in behavior, we reexamined (extending the experiments to 9 M perchloric and triflic acids) and reproduced the observations on the benzamido complex. In addition, we confirmed that the protonation is reversible. Another oddity is that for the benzamido and isonicotinamido complexes, there appear to be *two* bands associated with the amido chromophore, for example with benzamide, one at 314 nm and one at 393 nm. The lower energy band has the characteristics of a charge-transfer band.
(47) Curtis, J. C.; Sullivan, B. P.; Meyer, T. J. *Inorg. Chem.* **1983**, *22*, 224–236.
(48) Lever, A. B. P. *Inorganic Electronic Spectroscopy*, 2nd ed.; Elsevier: New York, 1984.
(49) Verdonck, E.; Vanquickenborne, L. G. *Inorg. Chem.* **1974**, *13*, 762–764.
(50) Waysbort, D.; Evenor, M.; Navon, G. *Inorg. Chem.* **1975**, *14*, 514–519.

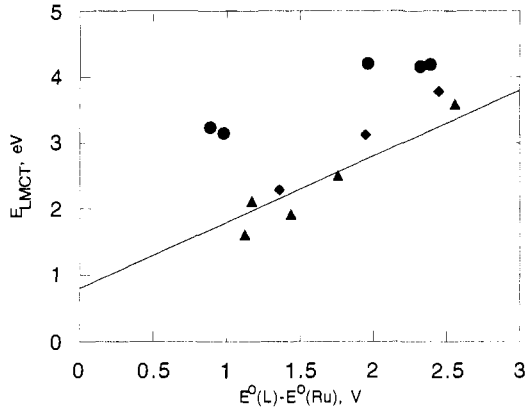

Figure 8. Plot of LMCT band energies (aqueous media) for $(NH_3)_5Ru^{III}(L^-)$ complexes against the differences in free $L^{0/-}$ and $(NH_3)_5Ru^{III/II}(L^-)$ reduction potentials. Key: triangles, **1–3**; diamonds, **4–8**; circles, **9–13** (numbers refer to entries in Table 8). The line of slope = 1 is drawn, not fit to the data.

are 1.80, 1.97, and 2.40 eV for I, Br, and Cl, respectively. These are 2–3 times greater than the ~0.8-eV intercept for the halides and pseudohalides.) Similarly, for a series of 17 substituted phenylcyanamide "pseudohalide" pentaammineruthenium(III) complexes elaborated by Crutchley and colleagues,[33,51] the correlation between E_{LMCT} and $E°(L/L^-) - E°(Ru^{III/II})$ is excellent (slope 0.89, intercept 0.61 eV, $R = 0.95$).[33] However, the carboxamido ligands (and, to a smaller extent, OH^- and RCO_2^-) lie significantly above the value to be expected from the oxidation potential of the free anionic ligand and data for the other systems plotted. This behavior is consistent with exceptionally strong πp-to-πd donation, such that the "LMCT" transition is no longer in the charge-transfer limit, but rather is more bonding-to-antibonding in character, reminiscent of the behavior of Ru(II) ammine complexes containing exceptionally strong π-accepting ligands (e.g. the *N*-Me pyrazinium ion).[52]

The Ru(II)–carboxamido complexes studied here exhibit intense bands in the near-UV–visible region (Table 5). These are most reasonably ascribed to metal-to-ligand charge transfer, with the acceptor moiety being the aromatic ring. An MLCT assignment is also appropriate for the 600-nm band of the carboxylate (Table 6). The parent amide $NH_2C(O)R$, R = 4-py-*N*-Me^+, is rather readily reduced ($E°$ = –0.91 V vs SCE in acetonitrile) comparable to the ligands *N*-$Mepz^+$ (–0.73 V[52]) and NC-4-py-*N*-Me^+ (–0.69 V[47]), for which long wavelength MLCT bands are also observed. However, in the complexes of the latter two ligands, the Ru(II) is in direct conjugation with the aromatic ring by attachment to pyrazyl or nitrile nitrogen and is not as strongly reducing as in the amido complexes because of π-back-bonding stabilization by the *N*-heterocycle or nitrile ligand ($E°(Ru^{III/II})$ +0.77 for the nitrile[47] complex). The half-width of the 695-nm band for L = NHC(O)-4-py-*N*-Me^+, is greater (5100 cm^{-1}) than those found for ligands with pyridyl/pyrazyl attachments (3000–4500 cm^{-1}),[52] consistent with a greater degree of charge transfer in the transition. The oscillator strength (f) of the MLCT band is 0.16 and the extent of delocalization of the Ru(II) electron density (with r = 5.7 Å) is $\alpha^2 = 0.031$, which may be compared with[52-54] α^2 values of 0.047–0.072 for the MLCT bands of $(NH_3)_5Ru^{II}$ complexes with pyridyl lead-in groups. (On the basis of its molar absorptivity, f for the carboxylate is about half that for the amide.) These observations indicate that significant interaction of Ru(II) with the aromatic ring can be mediated by the carboxamido group and add support to a significant contribution from resonance structure **IIM**. The wide range of MLCT band maxima observed as R is varied (reminiscent of $Fe^{II}(CN)_5L^{3-}$,[55] with L an aromatic N-heterocycle) suggests that the MLCT transitions of the amido complexes are more purely charge transfer in nature than found for the analogous series in which the Ru(II) is attached to the nitrogen of the aromatic heterocycle.[52] However, the K^{II}_{am} values (fifth row of Table 5) suggest some ground-state stabilization by π-back-donation.

Concluding Remarks. The affinities of both $(NH_3)_5Ru^{III}$ and $(NH_3)_5Ru^{II}$ for the (protonated) amide ligands are not great. The deprotonated ligand stabilizes the III oxidation state preferentially by 3–5 orders of magnitude. Interesting contrasts emerge for the two oxidation states: for the amido ruthenium(III) complexes strong πp–πd interaction between the amido lone pair and the partially vacant Ru(III) orbital produce a short Ru–N bond length and rather high-energy LMCT transition manifesting significant bonding-to-antibonding character. By contrast, for the ruthenium(II) complexes MLCT transitions that lie in a rather pure charge-transfer limit are observed.

Acknowledgment. We thank Dr. S. Seltzer for helpful comments, Dr. E. Fujita for determining the NMR spectra, Dr. B. Brunschwig for assistance with rapid spectral scanning, and Ms. E. Norton for determining ammonia. This research was carried out at Brookhaven National Laboratory under contract DE-AC02-76CH00016 with the U.S. Department of Energy and supported by its Division of Chemical Sciences, Office of Basic Energy Sciences.

Supplementary Material Available: Tables S1–S9, giving crystallographic data collection parameters, anion bond distances and angles, anisotropic thermal parameters for non-hydrogen atoms, calculated hydrogen atom positions, details of proposed hydrogen bonds, and positional parameters for the non-hydrogen atoms (22 pages). Ordering information is given on any current masthead page.

(51) Crutchley, R. J.; Naklicki, M. L. *Inorg. Chem.* **1989**, *28*, 1955–1958.
(52) Creutz, C.; Chou, M. H. *Inorg. Chem.* **1987**, *26*, 2995–3000.
(53) Zwickel, A. M.; Creutz, C. *Inorg. Chem.* **1971**, *10*, 2395–2399.
(54) Winkler, J. R.; Netzel, T. L.; Creutz, C.; Sutin, N. *J. Am. Chem. Soc.* **1987**, *109*, 2381–2392.
(55) Toma, H. E.; Malin, J. M. *Inorg. Chem.* **1973**, *12*, 1039–1045.